Available online at www.sciencedirect.com
ScienceDirect
Applied Catalysis B: Environmental 76 (2007) 123–134
APPLIED CATALYSIS B: ENVIRONMENTAL
www.elsevier.com/locate/apcatb

Surface characterization studies of TiO_2 supported manganese oxide catalysts for low temperature SCR of NO with NH_3

Padmanabha Reddy Ettireddy [a], Neeraja Ettireddy [a], Sergey Mamedov [b], Punit Boolchand [c], Panagiotis G. Smirniotis [a,*]

[a] *Chemical and Materials Engineering Department, University of Cincinnati, Cincinnati, OH-45221-0012, United States*
[b] *Horiba Jobin Yvon Inc., 3880 Park Avenue, Edison, NJ 08820, United States*
[c] *Department of ECECS, University of Cincinnati, Cincinnati, OH 45221-0030, United States*

Received 19 May 2006; received in revised form 27 April 2007; accepted 2 May 2007
Available online 6 May 2007

Abstract

A series of TiO_2 supported manganese oxide catalysts were prepared by wet-impregnation method for the low temperature selective catalytic reduction (SCR) of NO with ammonia as a reductant. A combination of various physico-chemical techniques such as N_2 physisorption, O_2 chemisorption, TPR, X-ray diffraction (XRD), X-ray photoelectron spectroscopy (XPS), and Raman were used to characterize the chemical environment of these catalysts. O_2 chemisorption and XRD results suggest that Mn exist in a well-dispersed state at below 16.7 wt.% of Mn on TiO_2 anatase (Hombikat), 7.5 wt.% on TiO_2 rutile (Kemira) and P-25 (80% anatase + 20% rutile), and in microcrystalline phase above these loading levels on respective support materials. These results also reveal that Mn interacts very well with pure anatase phase compared to rutile. XPS results of Mn/TiO_2 anatase (Hombikat) catalysts illustrated the presence of MnO_2 as a major phase (peak at 642.0 eV) along with Mn_2O_3 as the minor phase at lower loadings. The presence of Mn_2O_3 disappears at higher loadings. The characterization results indicated that the manganese oxide exists as an isolated species at very low loadings, highly dispersed state probably as two dimensional monolayer species at intermediate loadings, polymeric or microcrystalline form of manganese oxide at higher (above monolayer capacity) loadings was envisaged. The catalytic performance of various amounts of Mn loaded on different TiO_2 supported catalysts for low temperature SCR reaction at catalyst bed temperature 175 °C under power plant conditions using GHSV = 50,000 h^{-1} was studied. The catalyst with 16.7 wt.% Mn/TiO_2 anatase (Hombikat) was found to be highly active and selective catalyst for this reaction. The Raman studies acted as complimentary tool to XPS in order to characterize the manganese oxides (MnO, Mn_2O_3, Mn_3O_4, MnO_2). Raman data show that there is a strong interaction between the Mn oxides and the support, which is responsible for the impressive catalytic performance in comparison with other systems we investigated.

Keywords: TiO_2 anatase; TiO_2 rutile; MnO_2; XPS; Raman; Low temperature SCR; NO; NH_3

1. Introduction

Among the various non-catalytic and catalytic processes developed to eradicate NO_x, the selective catalytic reduction (SCR) of NO_x by ammonia in the presence of excess oxygen using V_2O_5/TiO_2 (anatase) with either WO_3 or MoO_3 [1–4] is by far the most important commercial process today for removing NO_x from flue gas. This is because the catalyst has high SCR activity and is resistant to SO_2 poisoning. The predominant form of titania used is anatase. The required operating temperature for the industrial catalyst described above is typically 300–400 °C. This makes it necessary to locate the SCR unit upstream of the desulfurization and particulate control devices immediately after the steam generator in order to avoid spending money to reheat the flue gas. However, this accelerates the catalyst deactivation through exposure to high concentrations of SO_2 and small particulates. This can be avoided by locating the SCR unit at the very end of the flue gas pollution abatement units where the flue gas is relatively clean as it passes through the scrubber and the electrostatic precipitator or bag-house [5]. The advantages of tail-end configurations include catalyst exposure to a relatively clean flue gas, more space to accommodate any changes in the power cycle or fuel, a decrease in catalyst volume and hence

* Corresponding author. Tel.: +1 513 556 1474; fax: +1 513 556 3473.
E-mail address: Panagiotis.Smirniotis@uc.edu (P.G. Smirniotis).

0926-3373/$ – see front matter © 2007 Elsevier B.V. All rights reserved.
doi:10.1016/j.apcatb.2007.05.010

cost as the result of the cleaner flue gas, and an increase in catalyst life. Some supported transition metal oxide catalysts have been investigated for the low temperature SCR reactions, which can be capable of operating in the low temperature range 80–250 °C. Amorphous chromia [6], carbon-supported vanadium [7,8], manganese [9] and copper [10,11] oxides, alumina supported manganese oxide [12], TiO_2 supported chromia [13], vanadium and copper-nickel oxides supported on titania and alumina monoliths [14], show high activity for NO reduction with NH_3 at low temperatures. Recently [15,16], our research group found that titania supported Mn-, Cu-, and Cr- were highly active for low temperature (80–250 °C) SCR of NO with NH_3. Among all, 20 wt.% Mn/TiO_2 Hombikat was extremely active at 120 °C.

This paper presents a systematic study of the effects of various loadings of Mn on different phases of TiO_2 supports by wet-impregnation method. In addition, these catalysts were characterized by using various physico-chemical techniques such as BET, O_2 chemisorption, XRD, XPS, Raman, TPR etc., to understand the structure, oxidation/reduction properties and possible metal-support interaction of the manganese oxide species and titania support.

2. Experimental section

2.1. Catalyst preparation

TiO_2 anatase (Hombikat UV 100 from Schtleben) was used as support material. As determined by N_2 adsorption, it had a specific surface area of 309 $m^2\,g^{-1}$, a pore volume of 0.37 $cm^3\,g^{-1}$, and an average pore diameter of 4.5 nm. Manganese nitrate ($Mn(NO_3)_2{\cdot}xH_2O$, 99.99%, Aldrich) was used as the source of manganese. The Mn loadings were selected from 5 to 28 wt.%. The Mn/TiO_2 catalysts were prepared by a solution-impregnation method, where the required amount of manganese nitrate was added to a 100-ml beaker containing 1.0 g of support in 50-ml deionized water. The excess water was then slowly evaporated on a water bath with continuous stirring. For comparison purpose, some amount of TiO_2 anatase (Hombikat) support alone was mixed in deionized water, and then water was evaporated with continuous heating and stirring. The residues, thus obtained were dried in an oven at 120 °C for 12 h, and ground to obtain homogeneous powder. Prior to the reaction studies, the powder was calcined at 250 °C for 4 h under continuous airflow (150 mL min^{-1}). Pure MnO_2 and Mn_2O_3 were also prepared by decomposing hydrous manganese nitrate at 420 and 680 °C, respectively. The same preparation procedure was used to prepare TiO_2 rutile (Kemira, 100% rutile) and Degussa P-25 (80% anatase + 20% rutile) supported manganese oxide catalysts.

2.2. BET surface area

BET surface area of the titania and manganese loaded titania catalyst powders were measured by nitrogen adsorption at −197 °C using Micromeretics Gemini surface area apparatus. Prior to analysis, 0.05–0.1 g of catalysts was degassed at 150 °C for 2 h under helium atmosphere. The adsorption isotherms of nitrogen were collected at −197 °C using approximately six values or relative pressure ranging from 0.05 to 0.99.

2.3. X-ray diffraction (XRD)

XRD was used to identify the crystal phases of titania loaded manganese catalysts. These studies were performed on a Siemens D500 diffractometer equipped with a monochromated CuK_α radiation source (wavelength 1.5406 Å). The catalysts were run 2θ ranging from 5 to 70° with step size 0.1° and time step 1.0 s to assess the crystallinity of the manganese loading. XRD phases present in the catalyst samples were identified using JCPDS powder data files.

2.4. H_2 temperature program reduction (TPR)

TPR experiments were carried out on a Micromeretics Autochem I 2910. Approximately 50 mg of sample without any previous pretreatment were tested by increasing the temperature from 50 to 800 °C. The reducing gas, a mixture of 10 vol.% H_2 in Ar, at a flow rate of 50 ml min^{-1}, was used to reduce the catalyst with continuous temperature ramp. The temperature was then kept constant at 800 °C until the signal of hydrogen consumption returned to the initial values. The amount of H_2 consumed by the catalyst sample in a given temperature range (in μmol g^{-1}) was calculated by integration of the corresponding TCD signal intensities.

2.5. Raman spectroscopy

Raman spectra of materials were taken with a Raman spectrometer (LabRam HR, Horiba Jobin Yvon Inc.) equipped with Olympus BX-41 microscope (objective ×100) and TE-cooled CCD detector (Andor), in a backscattering configuration using He-He laser (632.8 nm excitation line) with power of 5–10 mW at a sample and spectral resolution of 0.8 cm^{-1}.

2.6. X-ray photoelectron spectroscopy (XPS)

XPS was used to analyze the atomic surface concentration on each catalyst. The spectra were recorded on a Perkin-Elmer Model 5300 X-ray photoelectron spectrometer using MgK_α (1253.6 eV) as a radiation source at 300 W. The spectra were recorded in the fixed analyzer transmission mode with pass energies of 89.45 and 35.75 eV for recording survey and high-resolution spectra, respectively. The powdered catalysts were mounted onto the sample holder and degassed overnight at room temperature at a pressure on the order of 10^{-7} torr. Binding energies (BE) were measured for C 1s, O 1s, Ti 2p, and Mn 2p. Recorded Auger spectra for Mn was very weak. Sample charging effects were eliminated by correcting the observed spectra with the C 1s binding energy (BE) value of 284.6 eV. An estimated error of 0.1 eV can be considered for all the measurements. The spectra were smoothed, and a nonlinear background was subtracted.

2.7. Oxygen chemisorption

The dispersion of manganese on the support surface was determined by oxygen chemisorption measurements. These measurements were performed in a pulse (Micromeretics Autochemi I 2910 system) mode using He as carrier gas (30 STP cm^3 min^{-1}). Before analysis, approximately 50 mg of catalyst samples were reduced in flowing H_2 (50 STP cm^3 min^{-1}) at 250 °C for 2 h and then flushed at the same temperature for 30 min in the He carrier flow. Then oxygen pulses (1 ml loop volume) were injected onto the carrier gas until saturation of the sample was attained. The oxygen uptake was quantified by a TCD connected to a 2910 Autochem I (Micromeretics instrument). XRD, XPS results clearly indicated that most of the manganese oxide is in MnO_2 phase. Based on these results, the dispersion of manganese was expressed as the atomic ratio between oxygen and manganese content equal two (O/Mn = 2).

2.8. Catalytic experiments

The SCR of NO at atmospheric pressure was carried out in a fixed bed quartz reactor (i.d. 6 mm) containing calcined catalyst (80–120 mesh). Oxygen (Wright Bros., 4.00% in He), ammonia (Matheson, 4.06% in He) and nitric oxide (Air Products, 2.0% in He) were used as received. The reaction temperature 175 °C was measured by a type K thermocouple inserted directly into the catalyst bed. Experiments were performed at the GHSV 50,000 h^{-1}, the inlet concentrations of NO and NH_3 were each set at 400 ppm, and of O_2 remained constant (2 vol.%). The reactants and products were analyzed on-line using a Quadrapole mass spectrometer (MKS PPT-RGA), and a NO_x analyzer (Eco Physics CLD 70S). The NO conversion was explained based on the difference of in-let and out-let concentration of NO divided by in-let NO concentration, whereas N_2 selectivity was calculated based on the concentration of N_2 divided by the concentration of total products in the out-let of the reaction.

$$\text{NO conversion} = 100 \times (NO_{in} - NO_{out})/NO_{in} \quad (1)$$

$$N_2 \text{ selectivity} = 100 \times \{N_2/(N_2 + N_2O + NO_2)\} \quad (2)$$

3. Results and discussions

The BET surface area of the commercial TiO_2 anatase (Hombikat) sample obtained by N_2 physisorption at −193 °C was found to be 331 m^2 g^{-1}. In order to simulate the dopping process for the loading of the Mn, we exposed the titania to water followed by a calcination step at 240 °C for 4 h, the surface area dropped to 239 m^2 g^{-1}. It can be explained that the crystallinity and particle size of the support material increased after calcination. The BET surface area of various amounts of Mn loaded TiO_2 catalysts calcined at 240 °C are shown in Table 3. In the case of Mn loaded TiO_2 anatase (Hombikat) catalyst, a consistently decreasing trend with increasing Mn loading is noted in the series of the samples. In general the surface area of the catalyst material decreases with increasing quantity of the active component until the monolayer coverage of the impregnated component is completed [17]. However, in the case of TiO_2 rutile (Kemira) and TiO_2 (P-25) catalysts, the surface area is not changed much after calcination. The quantity of MnO_x needed to cover the support surface as a monomolecular layer can be estimated from structural calculations [18]. The monolayer surface coverage is defined as the maximum amount of MnO_x in contact with the oxide

Table 1
Summary of Mn/TiO_2 catalysts TPR results

Catalyst	T (°C)				H_2 consumption (μmole/g)	Change in average oxidation state
	T-1	T-2	T-3	T-4		
TiO_2 anatase (Hombikat)						
TiO_2 Calcined	405	591	–	–	–	–
5% Mn/TiO_2	261	368	472	–	1279.4	2.81
11.1% Mn/TiO_2	215	331	421	468	2148.4	2.36
16.7% Mn/TiO_2	209	294	409	463	2712.9	1.79
20% Mn/TiO_2	207	308	409	459	3061.9	1.68
24% Mn/TiO_2	212	300	407	467	3351.0	1.53
MnO_2	546	–	–	–	–	–
TiO_2 rutile (Kemira)						
TiO_2 Calcined	406	–	–	–	–	–
2.5% Mn/TiO_2	200	401	495	551	187.4	0.82
5% Mn/TiO_2	236	272	414	480	535.4	1.18
7.5% Mn/TiO_2	261	277	419	554	771.8	1.13
10% Mn/TiO2	277	287	412	554	1258.1	1.38
TiO_2 80% anatase; 20% rutile (P-25)						
TiO_2 Calcined	–	–	–	–	–	–
2.5% Mn/TiO_2	195	274	386	462	468.5	2.06
5% Mn/TiO_2	194	286	404	459	803.1	1.76
7.5% Mn/TiO_2	193	289	393	458	1075.2	1.58
10% Mn/TiO_2	193	292	396	459	1383.1	1.52

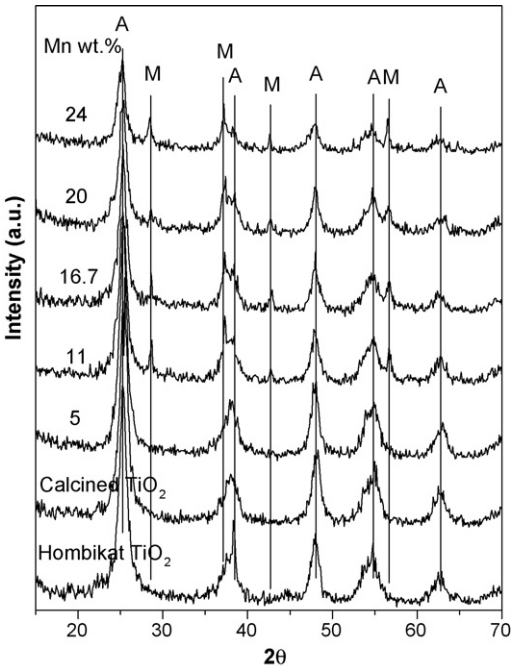

Fig. 1. XRD patterns of Mn/TiO_2 anatase (Hombikat) catalysts: (A) TiO_2 anatase; (M) MnO_2 phase.

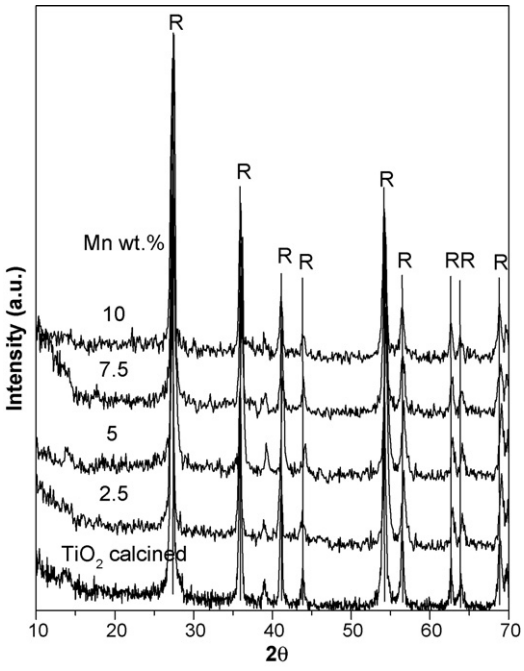

Fig. 2. XRD patterns of Mn/TiO_2 rutile (Kemira) catalysts: (R) Rutile.

support. From the M–O bond lengths of the crystalline Mn_2O_3, monolayer surface coverage is estimated to be 0.0532 wt.% Mn per m^2 of the support [18]. In reality, monolayer coverage depends not only on the support surface area but also on the concentration of reactive surface hydroxyl groups apart from other preparative variables [19]. In view of these reasons, a range of Mn loadings from 5 to 24 wt.% for TiO_2 anatase (Hombikat, 239 $m^2\ g^{-1}$), 2.5–10 wt.% for TiO_2 rutile (Kemira, 57 $m^2\ g^{-1}$), and 2.5–10 wt.% for TiO_2 P-25 (80% anatase + 20% rutile, 58 $m^2\ g^{-1}$) were selected in this investigation.

The X-ray powder diffraction patterns of Mn/TiO_2 anatase (Hombikat) catalysts of various Mn loadings calcined at 250 °C are shown in Fig. 1. Diffractograms of commercial TiO_2 anatase (Hombikat) and calcined TiO_2 alone are also included in Fig. 1. The XRD pattern of TiO_2 anatase (Hombikat) support appears to contain very sharp peaks at $d = 3.54$, 1.90, and 2.40 Å, which corresponds to anatase phase (JCPDS #71-1169). When the sample was calcined in air at 250 °C, its structure did not change. The Mn/TiO_2 samples with a Mn content 16.7 wt.% and above, calcined at 250 °C show X-ray reflections at $d = 2.41$, 1.63, and 2.11 Å (See Fig. 2) and its intensity increased gradually with the increase of the Mn loading. The appearance of XRD peaks at these d values is attributed to the formation of crystalline manganese oxide (MnO_2) phase (JCPDS # 04-0779). These results show that the XRD peaks of individual MnO_2 are absent up to 11 wt.% loading of manganese on titania anatase (Hombikat). This is a clear indication that manganese is in a highly dispersed state or the crystallites formed are less than 5 nm, and also insertion of manganese ions into the titania lattice [20] due to the presence of more surface hydroxyl groups in the titania anatase. Thus, up to 11 wt.% Mn on titania showed only the anatase phase of TiO_2. In addition, this result is in agreement with the theoretical monolayer capacity of TiO_2 support whose surface area is 237 $m^2\ g^{-1}$. This is further supported from and O_2 uptake data presented in later paragraphs. As shown in Fig. 2, the XRD patterns of Mn loaded TiO_2 rutile (Kemira) clearly shows that the TiO_2 rutile peak intensity was not changed even at 10 wt.% Mn loading. This demonstrates that the manganese oxide alone possibly dispersed as in the amorphous phase. Whereas in the case of Mn/TiO_2 P-25 catalysts the XRD peak intensity decreased (Fig. 3) with increase of Mn loading, and become complete amorphous at 10 wt.% Mn on TiO_2 P-25, which is what we observed in the case of TiO_2 anatase (Hombikat) catalysts. From these results we conclude that the Mn interacts very well with TiO_2 anatase compared to rutile phase.

Temperature programmed reduction (TPR) was used in the present study to investigate the oxidation states of different loadings of manganese deposited on the TiO_2 anatase (Hombikat) support and relate these oxidation states with activity studies of the catalysts. TPR profiles of various amounts of manganese loaded titania along with bulk MnO_2 and pure support are depicted in Fig. 4. The temperature at peak maximum (T-i) and the integral H_2 consumption in the temperature range 50–800 °C is summarized in Table 1. The reduction behavior of supported manganese catalysts mainly depends upon the inherent reducibility of the pure oxide supports because the support oxide determines the reactivity of the bridging Mn–O–Support functionalities [21]. Therefore, the reduction behavior of Mn deposited on the support surface is commonly not aligned to the reduction data of the bulk MnO_2. As shown in Fig. 4, the flat TPR profile of calcined TiO_2 support indicates that this support material itself is not reducible even at high temperatures. The pure MnO_2, treated in 10% H_2-in-Ar up to 800 °C, exhibited almost a one reduction peak [22]. It should

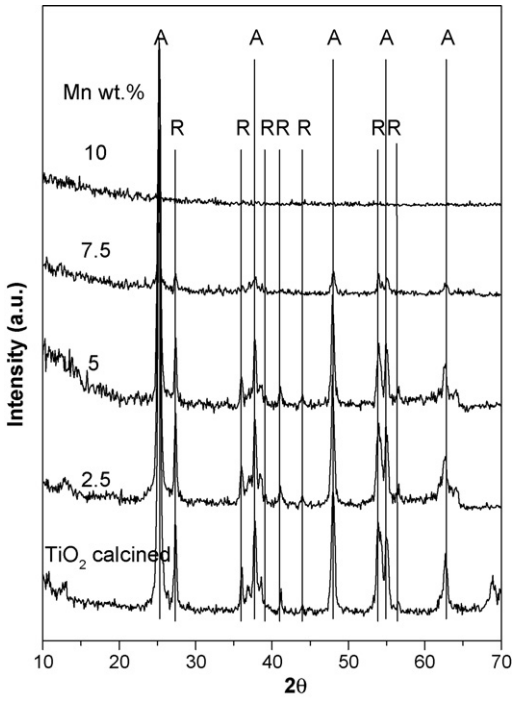

Fig. 3. XRD patterns of Mn/TiO_2 80% anatase and 20% rutile (P-25) catalysts: (A) anatase phase; (R) rutile phase.

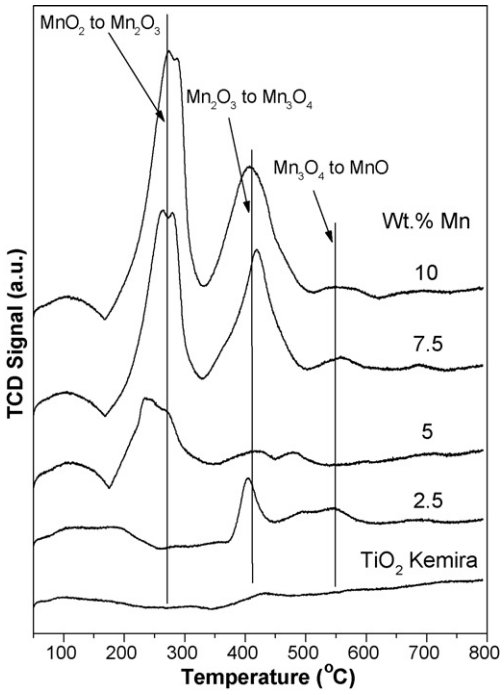

Fig. 5. TPR patterns of Mn/TiO_2 rutile (Kemira) catalysts.

be noted that the morphological properties of support materials (e.g., surface area, porosity), level of impurities (foreign compounds) as well as the method of preparation of MnO_2 may play an important role in determining the reducibility of MnO_2. The reduction of MnO_2 is influenced by the preparation procedure. In addition, the reduction temperature is also dependent on the reduction conditions, such as H_2 partial pressure and heating rate. It is, therefore, difficult to discuss the reduction temperature difference from the data obtained under different reduction conditions reported in the literature. The reported reduction temperatures are quite different, even for the same system in the literature. For example, Roozeboom et al. [23] have observed only a single reduction peak in their TPR of V_2O_5 studies, in contrast to the three multiple reduction peaks

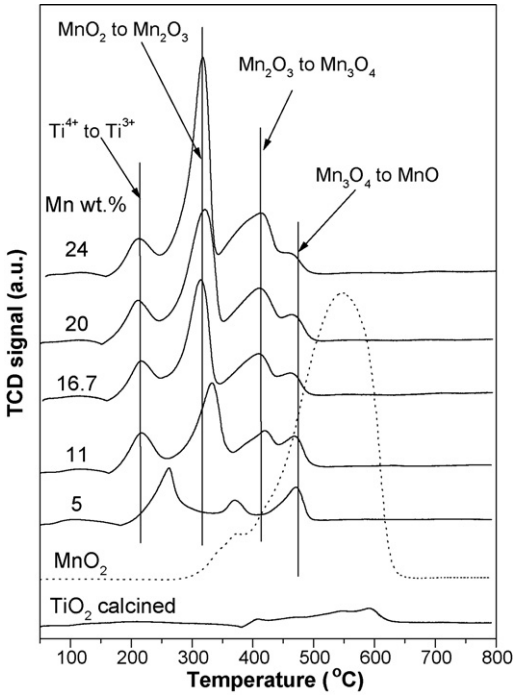

Fig. 4. TPR patterns of Mn/TiO_2 anatase (Hombikat) catalysts.

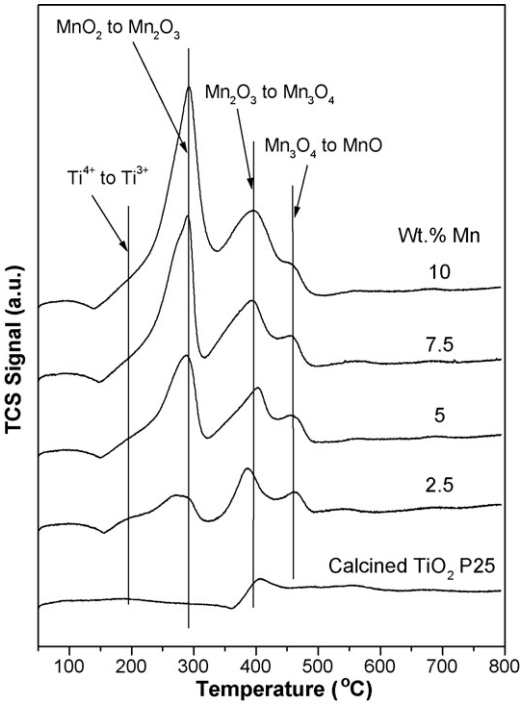

Fig. 6. TPR patterns of Mn/TiO_2 80% anatase and 20% rutile (P-25) catalysts.

seen by Bosch et al. [24]. In accordance with this trend, the reduction of bulk MnO_2 occurred at higher temperatures than titania supported manganese due to increased diffusional limitation in bulk MnO_2 (see Fig. 4 and Table 1).

Three reduction temperature peaks were observed in the range of 200–505 °C for 5% Mn/TiO_2 catalyst, which demonstrates the manganese oxide entered into the lattice structure of titania anatase. The first peak at 261 °C was due to the reduction of Ti^{4+} to $Ti^{3+}$and Mn^{4+} to Mn^{3+} because of interaction with titania and manganese oxide. This suggests that the low temperature reduction peak (*T*-1), in the TPR profile should be assigned to the support reduction due to the interaction with manganese oxide. The other two reduction peaks of these catalysts are attributed to the reduction of Mn_2O_3 to Mn_3O_4, and Mn_3O_4 to MnO. In addition to the first three reduction peaks *T*-1, *T*-2, and *T*-3, a new reduction peak *T*-4 appeared when manganese loading was increased from 11.1 to 24 wt.% (see Table 1). However, the *T*-2 reduction temperature for the catalysts with 16.67 and above wt.% Mn is somewhat different than that of 11.1 and 5 wt.% Mn/TiO_2 catalysts. This is due to the fact that at lower loading manganese is incorporated into the titania lattice. The reduction peaks for catalyst 11.1 wt.% Mn/TiO_2 catalysts emerged at 215, 331, 421, and 468 °C. As explained earlier the first peak at 215 °C is due to the reduction of Ti^{4+} to Ti^{3+} because of its interaction with manganese oxide. In the second reduction step, MnO_2 reduces to Mn_2O_3 at 331 °C, which further reduces to Mn_3O_4 and finally reached to MnO at 421 and 468 °C, respectively. For thermodynamic reasons further reduction of MnO does not occur under the applied experimental conditions [25]. The reduction peaks for catalysts with 16.67 wt.% and higher loadings of Mn have approximately the same positions as the peaks of the 11.1% Mn/TiO_2 catalysts. All these catalysts have temperature maximum 470 °C and the signal can be attributed to Mn_3O_4, which was due to the reduction of Mn_2O_3 to Mn_3O_4 and Mn_3O_4 to MnO. It is expected that at a lower temperature a surface-type (probably tetrahedral) species would be reduced, whereas at a higher temperatures a more polymeric or bulk like manganese oxide would be undergoing reduction. Arena et al. [26] studied MnO_x/TiO_2 catalyst prepared by impregnation of anatase sample with aqueous solution of $KMnO_4$ and calcined at 500 °C (11 wt.% Mn loading). Their TPR pattern shows main H_2 consumption at 383 °C and in high temperature region at 770 °C but without explanation about origin of such H_2 consumption. The intensity of total reduction peaks increased with the increase of manganese loading. As shown in Table 1, the total H_2 consumption decreased with increase of Mn loading, clearly indicates that the manganese oxide is dispersed well at the lower loadings. The change in average oxidation state of Mn (see Table 1), which was calculated from the total consumption hydrogen during the TPR process, continuously decreased with the increase of the manganese loading. This clearly demonstrates in Eq. (3) that the reduction process of Mn in presence of titania is assumed to take place accordingly [27]:

$$MnO_2 \rightarrow Mn_2O_3 \rightarrow Mn_3O_4 \rightarrow MnO \quad (3)$$

In addition to the TPR results, the X-ray diffraction data also showed the existence of MnO_2. This clearly indicates that manganese preferentially spreads on the titania anatase, up to monolayer coverage, before the formation of any bulk manganese oxide. The TPR results conclude that most of the manganese might have stabilized as Mn^{4+} oxidation state on the TiO_2 anatase support.

As shown in Fig. 5, the TPR reduction patterns for Mn loaded TiO_2 rutile (Kemira) displayed completely different than the TPR patterns of Mn/TiO_2 anatase (Hombikat), whereas Mn loaded on TiO_2 P-25 (80% anatase + 20% rutile) exhibited the same trend as was observed for the Mn/TiO_2 anatase (Hombikat) catalysts (Fig. 6), because of the presence of 80% anatase phase in the TiO_2 P-25 support. The TPR results indicate the interaction of MnO_x with TiO_2 anatase phase is stronger than the rutile phase. The reduction transition appeared at different temperature, a fact that can be explained due to the presence of different titania phases. The Mn/TiO_2 Kemira

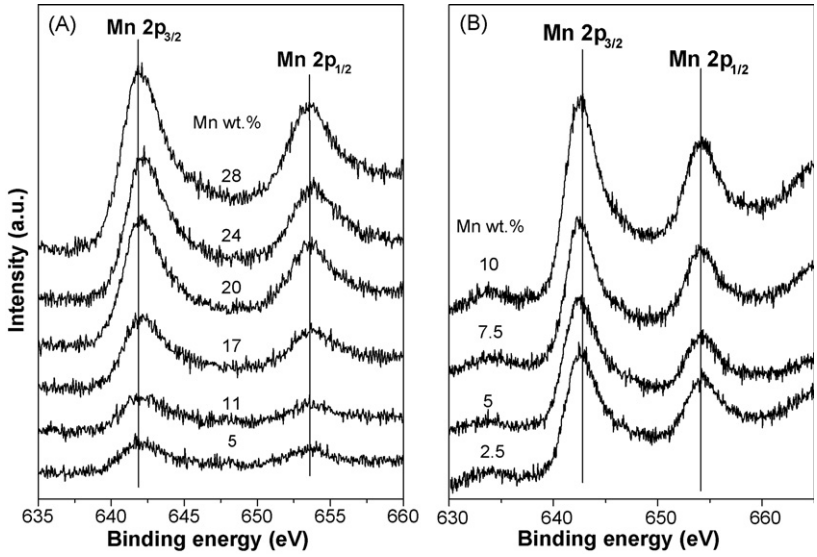

Fig. 7. XPS of Mn 2p core level peak for: (A) Mn/TiO_2 anatase (Hombikat) catalysts; (B) Mn/TiO_2 rutile (Kemira) catalysts.

catalysts consumed less hydrogen upto 7.5 wt.% of Mn compared to the corresponding Mn/TiO_2 P-25 catalysts. One can see another interesting results in Table 1, the average oxidation state of Mn on TiO_2 Kemira (100% rutile) increases with increase of Mn loading, whereas it is reverse in the case of Mn on TiO_2 P-25 (80% anatase and 20% rutile), which clearly indicates that the TiO_2 anatase phase interacts strongly with Mn up to 7.5 wt.% (monolayer coverage).

TiO_2 anatase (Hombikat) supported Mn catalysts were investigated by XPS to understand the surface atomic concentration and oxidation states of Mn interacting with titania on each catalyst. Fig. 7A shows the Mn 2p photoelectron peaks of the Mn/TiO_2 anatase (Hombikat) catalysts. A significant increase in the intensity and sharpening of Mn 2p peak can be noted with increasing Mn loading. The sharpening of XPS peak intensity can be attributed to various factors including: (1) the stabilization of only one type of Mn^{4+} oxidation state, which strongly interacted with the support surface; and (2) more electron transfer between the active component and the support (metal-support interaction). The binding energy values of Mn $2p_{3/2}$ for Mn/TiO_2 anatase (Hombikat) catalysts are depicted in Table 2. In all catalysts, the binding energy of Mn $2p_{3/2}$ is 642 eV; it probably corresponds to the Mn^{4+} state [28]. At lower loading, the XPS peak of Mn 2p appeared to be very broad with very small shoulders, which can be explained due the presence of different oxidation states of Mn along with major Mn^{4+}. This shoulder peak disappears at higher loadings. This result illustrated the presence of MnO_2 as a major phase along with Mn_2O_3 as the minor phase at lower loadings. It can also be explained that the Mn in the Mn^{4+} oxidation state is strongly interacted with TiO_2 anatase support. Due to this interaction, 16.67 wt. % Mn/TiO_2 catalyst gave high activity and selectivity towards low temperature SCR of NO with NH_3 reaction, which is discussed in the following paragraphs.

Fig. 7B and Table 2 show the binding energy values of Mn 2p core level spectra, which agree with the values reported in the literature [28]. It can be noted from this table that the core level binding energy is stable in all Mn loaded TiO_2 rutile (Kemira) catalysts. Very interestingly, the intensity of the Mn 2p line significantly increased with increasing Mn loading. This increase is more prominent in the case of 10 wt.% Mn/TiO_2 rutile (Kemira), indicating that the intensity of Mn 2p photoelectron signals depends on the coverage of Mn on the TiO_2 rutile (Kemira) carrier. The stable binding energy of Mn 2p suggests that the MnO_2 species stabilized in all catalysts. The same phenomenon was observed in the case of Mn/TiO_2 anatase (Hombikat) catalysts. One can observe that the difference in binging energy between Mn $2p_{3/2}$ and Mn $2p_{1/2}$ is larger in the case of Mn loaded TiO_2 rutile (Kemira) than in the case of Mn loaded TiO_2 anatase (Hombikat). This clearly indicates that the interaction of Mn is different on different support materials, even though the oxidation state of Mn is same in both the cases.

The relative dispersion of manganese on support surface was also estimated from XPS measurement of Mn/TiO_2 anatase (Hombikat) and Mn/TiO_2 rutile (Kemira) catalysts. The surface atomic concentrations of Mn 2p, Ti 2p, and Mn/Ti ratio for both types of catalysts are shown in Fig. 8A, B and Table 2. The intense signal corresponding to the Mn $2p_{3/2}$ level of manganese was compared with the Ti $2p_{3/2}$ level. The M 2p/Ti 2p ratio can be taken as a measure of the relative dispersion of manganese oxide on the support surface (see Fig. 8A and B). As can be noted, the surface atomic concentration of Mn increased and Ti decreased with increase of Mn loading in the case of Mn/TiO_2 anatase (Hombikat) catalysts (Fig. 8A); whereas the surface atomic concentration of both Mn and Ti increased initially for loadings up to 7.5 wt.%, and then surface atomic concentration of Ti alone decreased at 10 wt.% Mn (Fig. 8B) in the case of Mn/TiO_2 rutile (Kemira). But the increase in surface atomic concentration of Mn is more predominant compared to the Ti (Fig. 8B). In general, the surface atomic ratio of Mn/Ti is increased with the increase of Mn loading, which indicates that support surface is covered by manganese oxide (Fig. 8A and B).

The surface atomic ratio of Mn/Ti clearly explains that the Mn is intercalated in the TiO_2 anatase (Hombikat) lattice structure at lower loadings due to high surface and smaller

Table 2
Binding energy surface atomic ratio between Mn 2p and Ti 2p for Mn/TiO_2 catalysts determined from XPS analysis

Catalyst	Binding energy (eV)					Mn/Ti
	Ti $2p_{3/2}$	Ti $2p_{1/2}$	O 1s	Mn $2p_{3/2}$	Mn $2p_{1/2}$	
TiO_2 anatase (Hombikat)						
TiO_2	458.5	464.2	529.6	642.0	653.7	0
5%Mn/TiO_2	458.5	464.2	529.7	642.1	653.7	0.10
11.1% Mn/TiO_2	458.5	464.2	529.8	642.0	653.7	0.13
16.7% Mn/TiO_2	458.5	464.2	529.7	642.0	653.7	0.28
20% Mn/TiO_2	458.5	464.2	529.8	642.0	653.7	0.54
24% Mn/TiO_2	458.5	464.2	529.8	642.0	653.7	0.63
TiO_2 rutile (Kemira)						
TiO_2	458.5	464.2	530.0	–	–	0
2.5%Mn/TiO_2	458.5	464.2	530.2	642.1	654.1	0.63
5% Mn/TiO_2	458.5	464.2	530.2	642.0	654.1	0.71
7.5% Mn/TiO_2	458.5	464.2	530.2	642.0	654.1	0.82
10% Mn/TiO_2	458.5	464.2	530.2	642.0	654.1	1.16

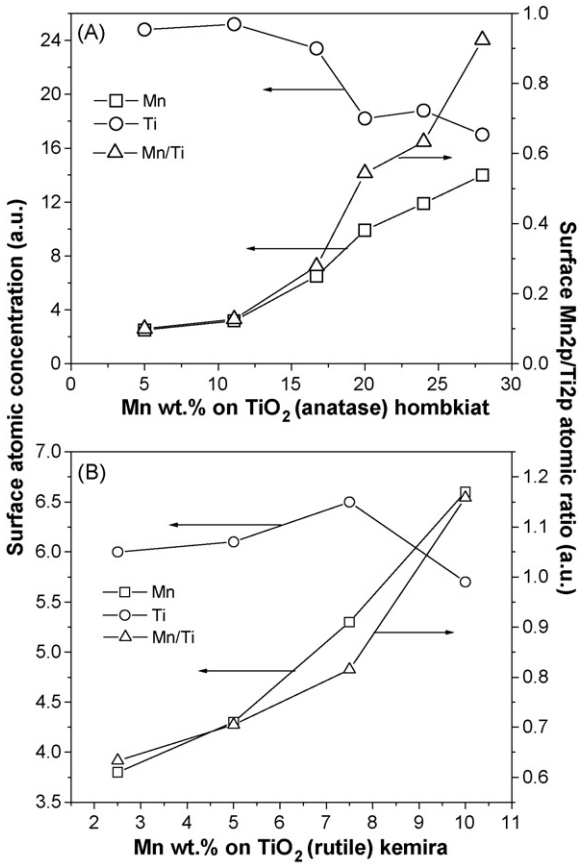

Fig. 8. Surface atomic concentration of Mn 2p, Ti 2p and surface atomic ratio between Mn 2p and Ti 2p obtained from XPS analysis: (A) Mn/TiO_2 anatase (Hombikat) catalysts; (B) Mn/TiO_2 rutile (Kemira) catalysts.

particle size of the support. Because of this reason, Mn is highly dispersed at a certain level called two-dimensional monolayer coverage. After reaching this level, the surface atomic ratio of Mn/Ti increased significantly on further loadings of Mn. This can be explained due to the formation of microcrystalline Mn oxide species formed on the support surface at higher loadings. XPS results clearly demonstrated that the completion of monolayer coverage takes place at approximately 16.7 and 7.5 wt.% Mn for Mn/TiO_2 anatase (Hombikat) and Mn/TiO_2 rutile (Kemira) catalysts, respectively. The results indicated that the manganese oxide exists as an isolated species at very low loadings, highly dispersed state probably as two dimensional monolayer species at intermediate loadings, polymeric or microcrystalline form of manganese oxide at higher (above monolayer capacity) loadings was envisaged. These results are in perfect agreement with XRD and TPR results that we discussed in earlier paragraphs.

Raman spectra of Mn/TiO_2 are shown in Fig. 9A–C. All Mn oxides are light sensitive [29] and we used very low laser power (5–10 mW) to avoid degradation and local heating. This point should be considered with particular attention since local heating can cause misleading shifts and broadening of the Raman modes. The peaks of Mn_2O_3 and MnO_2 located around 600–650 cm^{-1} are overlapped with strong band of TiO_2 in this region (Fig. 9). Raman pattern of TiO_2 Hombikat support clearly showed anatase crystalline structure. The anatase

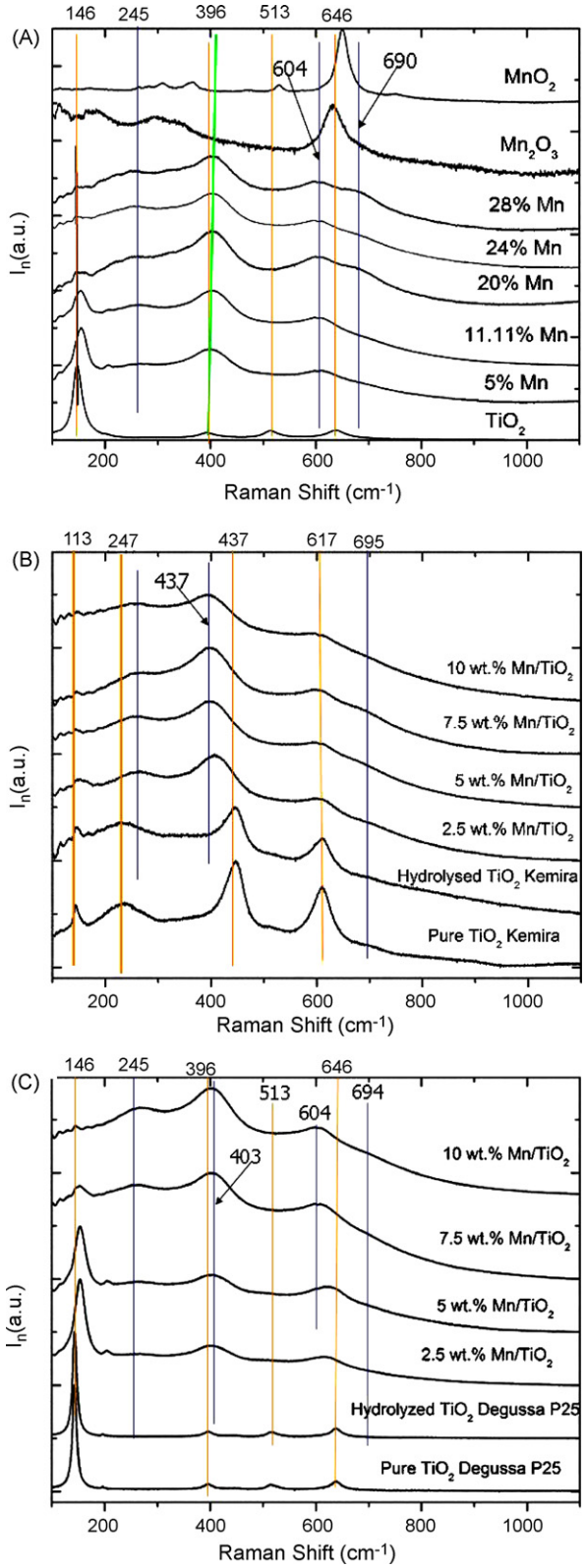

Fig. 9. A: Raman spectra of Mn/TiO_2 anatase (Hombikat) catalysts. B: Raman spectra of Mn/TiO_2 rutile (Kemira) catalysts. C: Raman spectra of Mn/TiO_2 80% anatase and 20% rutile (P-25) catalysts.

structure is tetragonal, and its conventional cell is composed by two primitive cells, each with two TiO_2 units and its space group is D_{4h}^{19}. The six modes A_{1g} 519 cm^{-1}, $2B_{1g}$ 399 cm^{-1} and 519 cm^{-1}, and $3E_g$ 144 cm^{-1}, 197 cm^{-1}, and 639 cm^{-1} are Raman active. Our primary interest is the peak at 144 cm^{-1} and it corresponds to E_g mode of anatase. The Mn/TiO_2 samples show that this peak gradually decreases in intensity, becomes broader and shifts to the high frequency region with increase of Mn loading and disappeared at the concentration of Mn-oxide above 11%. The peak position and broadening compare to the larger crystalline size samples can be explained by finite size crystal using quantum confinement effect. In an ideal and infinite single crystal, only phonons near the center of the Brillouin zone contribute to the Raman spectrum because of momentum conservation between phonons and incident as well as scattered light. In addition, in fine crystals, phonons can be confined in space by crystal boundaries, and this condition produces an uncertainty in the wave vector $\Delta q = 2\pi/L$, where L is the correlation length of the phonon (or crystalline size in an ideal case), allowing phonons with $q \neq 0$ to contribute to the Raman spectrum. Unfortunately, the phonon dispersion curve of anatase has not yet been obtained experimentally or theoretically, and we cannot extend the discussion in a quantitative way at this stage. Quantum confinement effect has been recently examined by comparison size of the nanocrystals and width of the Raman band and it was shown a good correlation [30]. At low loading, Mn-oxide is form monolayer structures with Mn atoms incorporated to the crystalline lattice. It generates distortion of the crystalline lattice and, therefore, confinement effect. At concentration above 11% Mn-oxide form microcrystalline species. Because Raman cross section of Mn-oxide is relatively low, spectra becomes very weak. Raman results clearly show that formation of micro crystals on the surface occurs at 11 (and more) and 7.5 wt.% (and more) for Hombikat and Kemira, respectively. These data are in an excellent agreement with above-mentioned XRD, TPR and XPS results.

Dispersion is normally controlled by the extent of loading, nature of support and active component, and the method of preparation. To determine the dispersion of metal catalysts, the most commonly used and widely accepted method is selective chemisorption of suitable gases like hydrogen and carbon monoxide. Parekh and Weller [31,32] have devised a simple oxygen chemisorption method for determining the dispersion of equivalent molybdena area of MoO_3/Al_2O_3. The choice of temperature at which oxygen chemisorption could give meaningful information about the surface structure of supported metal oxide catalysts was deemed crucial. On the basis of the observation made by these researchers, it was proposed that −196 °C (and later on −78 °C) is the most suitable temperatures for oxygen chemisorption measurements. Subsequently, Oyama et al. [21] have proposed that if the temperature of oxygen chemisorption is around 370 °C with a pre-reduction of the catalysts at the same temperature, results would give much more meaningful information than the results generated at −78 °C with a pre-reduction of the sample at 500 °C temperature. Reddy et al. [33] have also reported that the oxygen uptake measured at 370 °C with a pre-reduction of the sample at the same temperature probably avoids bulk and over reduction of vanadium oxide and sintering of the support material. The pre-reduction temperature of catalysts was selected at 250 °C for O_2 pulse chemisoprtion experiments in order to start with the surface reduction of support and active component. The first reason, these catalysts were calcined at low temperature, and also active for low temperature (below 200 °C) SCR of NO reduction. Second reason, as shown in TPR patterns of all catalyst, the first reduction temperature peak appeared at below 250 °C related to the reduction of surface interacted support and active bridge (Ti–O–Mn) component, which is very important for the activity of the catalyst. Third reason, Oyama et al. [21] have proposed that the oxygen uptake and the pre-reduction of the catalysts at the same temperature, would give much more meaningful information than the results generated by catalyst pre-reduced at different temperatures. Therefore, for our catalyst system, we have selected 250 °C as the pre-reduction and O_2 pulse chemisorption temperature which gives momentous information for supported Mn based catalyst systems.

Oxygen uptake values obtained at 250 °C on various Mn/TiO_2 samples are presented in Table 3. Under experimental conditions employed in this study, the pure support seems to chemisorb very small amount of oxygen. Therefore, the contribution of the pure support was subtracted from the uptake results. As seen in Table 3, the oxygen uptake value drastically increases with increasing in the manganese content up to 16.7 wt.% Mn loading and then approaches limiting value with further increase in loading. This saturation level is an indication of completion of monolayer coverage of manganese on the support surface. Whereas in the case of other two types of titanias such as TiO_2 rutile (Kemira) and TiO_2 80% anatase, 20% rutile (P-25) supported manganese catalysts, the oxygen uptake value significantly increased up to 7.5 wt.%, then the increase in oxygen uptake value is slow at 10 wt.% Mn-loading. As we discussed in later paragraphs, the dispersion of Mn at 7.5 wt.% is higher than the 10 wt.% Mn catalysts. This clearly indicates the 7.5 wt.% of Mn is the nearest monolayer coverage on the these support materials.

The dispersion, defined as the percent of Mn-oxide units available for reduction and subsequent oxygen uptake, is estimated from the total number of Mn-oxide units present in the sample and the number of oxygen atoms chemisorbed (Table 3). The dispersion is found to increase with the increase in Mn loading up to 16.7 wt.% and started decreasing beyond this loading thus, suggesting that the Mn is dispersed as an isolated species at lower loadings, two-dimensional monolayer coverage near or just below 16.7 wt.% and dimeric or paracrystalline or microcrystalline phase at higher loadings. This is, of course, a general phenomenon with any supported metal oxide catalyst systems [33]. As shown in Table 3, the dispersion values for Mn/TiO_2 rutile (Kemira) and Mn/TiO_2 80% anatase + 20% rutile (P-25) catalysts increased up to 7.5 wt.% and decreased at 10 wt.% Mn loading, which clearly indicates that the doping of Mn on TiO_2 rutile phase cannot follow a theorical monolayer calculation rule. The results

Table 3
BET surface area, oxygen uptake, metal dispersion and TOFs of Mn/TiO_2 catalysts

Catalyst	BET surface area (m^2/g)	O_2 uptake[a] ($\mu mol\ g_{cat}^{-1}$)	Dispersion[b] (%)	Site density[c] ($10^{17}/m^2$)	TOF[d] at different GHSV (h^{-1})		
					50000	100000	150000
TiO_2 anatase (Hombikat)							
TiO_2	328	0.00	0	0	0	0	0
TiO_2 calcined	239	0.00	0	0	0	0	0
5% Mn/TiO_2	238	212	46.4	5.37	139.5	127.8	107.6
11.1% Mn/TiO_2	229	508	50.4	13.36	60.1	58.7	49.3
16.7% Mn/TiO_2	196	882	58.0	27.10	32.3	31.7	26.3
20% Mn/TiO_2	183	928	50.8	30.54	27.8	27.5	26.3
24% Mn/TiO_2	165	1022	43.8	37.31	22.0	21.3	21.1
TiO_2 rutile (Kemira)							
TiO_2 calcined	54	0.0	0.00	0	0	–	–
2.5% Mn/TiO_2	54	50	21.6	5.57	53.5	–	–
5% Mn/TiO_2	55	210	46.0	22.99	31.8	–	–
7.5% Mn/TiO_2	51	416	60.8	49.13	17.1	–	–
10% Mn/TiO_2	49	522	57.2	64.16	12.8	–	–
TiO_2 80% ananase; 20% rutile (P-25)							
TiO_2 calcined	52	0.0	0	0	0	–	–
2.5% Mn/TiO_2	51	124	54.0	14.64	40.1	–	–
5% Mn/TiO_2	51	292	64.0	34.48	19.9	–	–
7.5% Mn/TiO_2	49	450	67.6	55.31	13.1	–	–
10% Mn/TiO_2	49	544	59.6	66.87	11.7	–	–

[a] Pretreatment and O_2 uptake temperature is 250 °C.
[b] Dispersion: fraction of Manganese atoms at the surface.
[c] Oxygen atom site density: number of oxygen atom chemisorbed per m^2 of surface.
[d] TOF: number of NO molecules converted per specific oxygen atom site per hour.

obtained from oxygen chemisorption technique are in perfect agreement with the XRD, TPR, and XPS results described in the earlier paragraphs. As a result, valuable information like oxygen uptake and metal-dispersion and change in oxidation states of manganese can be obtained from the simple oxygen pulse chemisorption technique.

The catalytic performance of various amounts of Mn loaded on different phase of TiO_2 catalysts were tested for low temperature SCR at reaction temperature 175 °C. As reported in our earlier work MnO_x/TiO_2 provides respectable catalytic activity relative to the other transition metals tested at temperatures below 150 °C [15,16]. Since SCR catalysts used in power plants will typically see usage above 30,000 h^{-1}, all of the catalysts previously discussed were tested at 50,000 h^{-1}. The NO conversion and N_2 selectivity results on the above mentioned catalysts were presented in Figs. 10–12. The NO and NH_3 conversions were zero when TiO_2 anatase (Hombikat) alone was used as catalysts (Fig. 10). As the manganese content increases on the support surface, the NO conversions and N_2 selectivity increased up to 16.67 wt.% Mn and then decreased for higher loading level. However, the NH_3 conversion increased with increase of Mn loading. The increasing of NH_3 conversion at higher loadings manganese makes the decrease in NO conversion and N_2 selectivity. These results clearly indicate that the conversion and N_2 selectivity is strongly dependent on the dispersion of manganese on the support surface. In other words, for obtaining better yields of N_2 a high concentration of manganese equivalent to the monolayer capacity and above on the support surface is highly essential. As can be noted from the Fig. 10, high conversion of NO (94%) with 100% selectivity towards N_2 is achieved on the 16.67 wt.% Mn/TiO_2 Hombikat. Very interestingly, this composition is exactly corresponding to the near or just above the monolayer capacity of Mn on the TiO_2 anatase (Hombikat) support. As we already mentioned in the O_2 uptake results, the amount of manganese to achieve a monolayer coverage on a given support material can be estimated to be 0.0532 wt.% Mn per m^2 of the support [18]. In fact, a direct relationship was found to exist between oxygen uptakes and total conversion of NO at all Mn loadings. The catalytic performance of Mn/TiO_2 rutile (Kemira) showed (Fig. 11) exactly the same trend that was

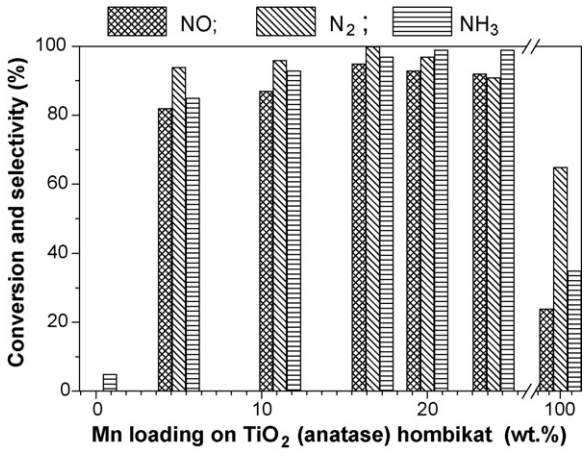

Fig. 10. Catalytic performance of Mn/TiO_2 anatase (Hombikat) catalysts: NH_3 = 400 ppm; NO = 400 ppm, O_2 = 2.0 vol.%; GHSV = 50,000 h^{-1}; catalyst wt. = 100 mg; reaction temperature = 175 °C.

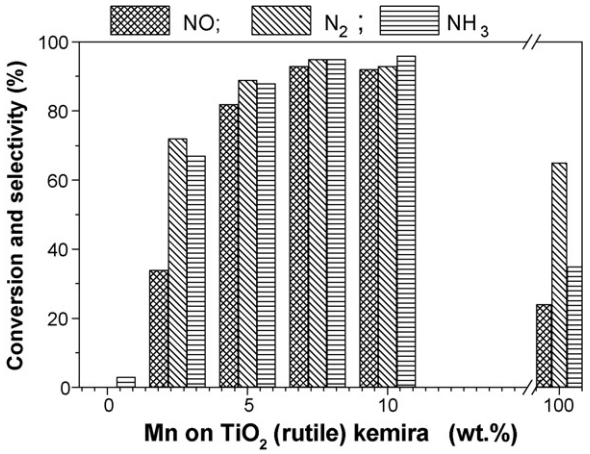

Fig. 11. Catalytic performance of Mn/TiO_2 rutile (Kemira) catalysts: NH_3 = 400 ppm; NO = 400 ppm; O_2 = 2.0 vol.%; GHSV = 50000 h^{-1}; catalyst wt. = 100 mg; reaction temperature = 175 °C.

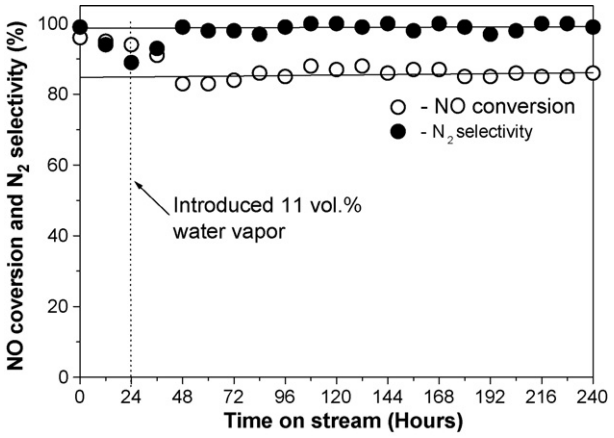

Fig. 13. Time-on-stream behavior of 16.7 wt.% Mn/TiO_2 anatase (Hombikat) catalyst in the absent and presence of the 11 vol.% water vapor: NH_3 = 400 ppm; NO = 400 ppm; O_2 = 2.0 vol.%; GHSV = 50,000 h^{-1}; catalyst wt. = 100 mg; reaction temperature = 175 °C.

observed with Mn/TiO_2 anatase (Hombikat) catalysts. However, we never observed the selectivity of N_2 to reach 100% in this case. This can be explained because the interaction of Mn with rutile phase of TiO_2 is not as good as with the anatase phase of TiO_2. As shown in Fig. 12, Mn/TiO_2 (P-25) is not as active as other two catalysts under identical operating conditions. This result is expected because the TiO_2 P-25 support material contains two types of titania phase, which cannot allow to disperse Mn properly on its surface. Even though the support material contains 80% of anatase phase, the particle size of this support is far bigger than that of TiO_2 anatase (Hombikat) support.

Additionally, industrial SCR units are exposed to significant amounts of water from combustion. As reported in the earlier work [16] Cu/TiO_2 provided high catalytic activity at 50,000 h^{-1} and max out in activity from 200 °C. Manganese on TiO_2 was clearly most useful at temperatures below 150 °C, as its N_2 selectivity quickly declines below 95% as the temperature increases [15]. It appears that Cu/TiO2 outperforms Mn/TiO2 at higher space velocities when both the activity and selectivity data are considered; however, SCR units in power plants must have N_2 selectivities above 95% to avoid releasing significant amounts of N_2O into the atmosphere. Consequently, the catalytic performance of all the supported transition metal oxides tested in the presence of 11 vol.% water vapor [15]. Among all, Mn/TiO_2 provided the best overall performance when water is present. Therefore, the time-on-stream behavior of this catalyst before and after 11 vol.% water vapor was tested for 10 days (See Fig. 13). The NO conversion and N_2 selectivity of the catalyst in the absence of water decreased with time. As shown in Fig. 13, the introduction of water vapor after 24-h time-on-stream study drastically increased the selectivity of N_2 with slow decreasing of NO conversion. After certain time, the NO conversion and N_2 selectivity stabilized for throughout the time-on-stream study. This suggests that water preferentially adsorbs on the active sites responsible for the N_2O formation, and this phenomenon is beneficial for the application of Mn/TiO2 catalysts in power plants.

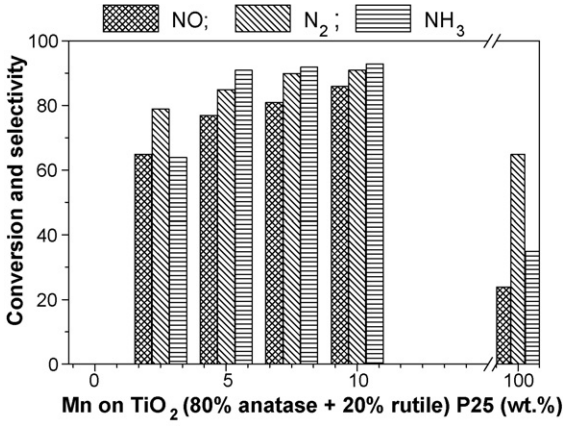

Fig. 12. Catalytic performance of Mn/TiO_2 80% anatase and 20% rutile (P-25) catalysts: NH_3 = 400 ppm; NO = 400 ppm; O_2 = 2.0 vol.%; GHSV = 50,000 h^{-1}; catalyst wt. = 100 mg; reaction temperature = 175 °C.

4. Conclusions

Among three different types of titanias, TiO_2 anatase (Hombikat) supported 16.7 wt.% Mn catalyst is the best one for low temperature SCR of NO with NH_3. This catalyst offers 94% NO conversion, 96% NH_3 and 100% N_2 selectivity. Monolayer coverage of manganese oxide on different titania supports was determined by the most of characterization techniques such as oxygen chemisorption, XRD, XPS, Raman, and TPR. The results indicate that the completion of monolayer coverage takes place at near 16.7 wt.% Mn loading. One can conclude that results obtained from characterization techniques, the manganese oxide exists as an isolated species at very low loadings, highly dispersed state probably as two dimensional monolayer species at intermediate loadings, polymeric or microcrystalline form of manganese oxide at higher (above monolayer capacity) loadings was envisaged.

The following are the additional conclusions from this study:

1. The TiO_2 anatase appears to be a promising support material for dispersion of manganese oxide.
2. Highly dispersed Mn-oxide monolayer catalysts with Mn loadings nearly equivalent to theorical monolayer capacity of the support material can be obtained when TiO_2 anatase is used as a support material.
3. The Mn/TiO_2 anatase catalyst is very active for low temperature SCR of NO with NH_3 in comparison to other titanias supported Mn catalysts.
4. The time of stream study of the Mn/TiO_2 anatase catalyst showed stable NO conversion and N_2 selectivity even for 10-days time-on-stream in the presence of 11 vol.% water vapor at 175 °C.

Acknowledgments

The authors are grateful to acknowledge National Science Foundation (NSF) for supporting this work through the Grant # CTS-0237172, and allowing us to publish the findings. The authors wish to thank Dr. Maruthi Sreekanth Pavani for very fruitful discussions on this work.

References

[1] F. Janssen, F. Van den Kerkhof, H. Bosch, J.R.H. Ross, J. Phys. Chem. 91 (1987) 5921.
[2] G. Ramis, G. Busca, F. Bregani, Catal. Lett. 18 (1993) 299.
[3] S.C. Wood, Chem. Eng. Progr. 90 (1994) 32.
[4] J.A. Dumesic, N.-Y. Topsoe, H. Topsoe, T. Slabiak, J. Catal. 163 (1996) 409.
[5] J.N. Armor, Environmental Catalysis 205th National ACS Meeting, 1994, p. 206.
[6] H.E. Curry-Hyde, H. Musch, A. Baiker, Appl. Catal. 65 (1990) 211.
[7] S. Kasaoka, E. Sasaoka, H. Iwasaki, Bull. Chem. Soc. Jpn. 62 (1989) 1226.
[8] Z. Zhu, Z. Liu, S. Liu, H. Niu, T. Hu, T. Liu, Y. Xie, Appl. Catal. B 26 (2000) 25.
[9] M. Yoshikawa, A. Yasutake, I. Mochida, Appl. Catal. B 17 (1998) 239.
[10] F. Nozaki, K. Yamazaki, T. Inomata, Chem. Lett. (1977) 521.
[11] L. Singoredjo, M. Slagt, J. van Wees, F. Kapteijn, J.A. Moulijn, Catal. Today 7 (1990) 157.
[12] L. Singoredjo, R. Korver, F. Kapteijn, J.A. Moulijn, Appl. Catal. B 10 (1996) L237.
[13] H. Schneider, M. Maciejewsk, K. Köhler, A. Wokaun, A. Baiker, J. Catal. 157 (1995) 312.
[14] J. Blanco, P. Avila, S. Suárez, J.A. Martín, C. Knapp, Appl. Catal. B 28 (2000) 235.
[15] P.G. Smirniotis, D.A. Peña, B.S. Uphade, Angew. Chem. Int. Ed. Engl. 40 (2001) 2479.
[16] D.A. Peña, B.S. Uphade, P.G. Smirniotis, J. Catal. 221 (2004) 431.
[17] F.E. Massoth, Adv. Catal. 27 (1978) 265.
[18] J.M.G. Amores, T. Armaroli, G. Ramis, F. Finaochio, G. Busca, Appl. Catal. B 22 (1999) 259.
[19] G.C. Bond, S.F. Tahir, Appl. Catal. 71 (1991) 1, and references therein.
[20] G. Pechi, P. Reyes, T. Lopez, R. Gomez, A. Moreno, J.L.G. Fierro, J. Chem. Technol. Biotechnol. 77 (2002) 944.
[21] S.T. Oyama, G.T. Went, K.B. Lewis, A.T. Bell, G.A. Somorjai, J. Phys. Chem. 93 (1989) 6786.
[22] E.R. Stobbe, B.A. de Boer, J.W. Geus, Catal. Today 47 (1999) 167.
[23] F. Roozeboom, M.G. Mittlemeijer-Hardeger, J.A. Mouljin, J. Medma, U.H.J. de Beer, P.J. Gellings, J. Phys. Chem. 84 (1980) 2783.
[24] H. Bosch, B.J. Kip, J.G. van Ommen, P.J. Gellings, J. Chem. Soc. Faraday Trans. I 80 (1984) 2479.
[25] I.R. Leith, M.G. Howden, Appl. Catal. 37 (1988) 75.
[26] F. Arena, T. Torre, C. Raimondo, A. Parmaliana, Phys. Chem. 3 (2001) 1911.
[27] J. Carno, M. Ferradon, E. Bjornbom, S. Jaras, Appl. Catal. A 155 (1997) 265.
[28] F. Kapteijn, J. Dick van Langeveld, J.A. Mouljin, A. Andreini, M.A. Vuurman, A.M. Turek, J.-M. Jehng, I.E. Wachs, J. Catal. 150 (1994) 94.
[29] M.-C. Bernard, A.H. Goff, Bich Vu Thi, S.C. de Terresi, J. Electrochem. Soc. 140 (1993) 3065.
[30] A. Li Bassi, D. Cattaneo, V. Russo, C.E. Bottani, E. Barborini, T. Mazza, P. Piseri, P. Milani, F.O. Ernst, K. Wegner, S.E. Pratsinis, J. Appl. Phys. 98 (2005) 074305.
[31] B.S. Parekh, S.W. Weller, J. Catal. 47 (1977) 100.
[32] S.W. Weller, Acc. Chem. Res. 16 (1983) 101.
[33] B.M. Reddy, B. Manohar, E.P. Reddy, Langmuir 9 (1993) 1781.